Am J Transl Res 2023;15(2):779-798
www.ajtr.org /ISSN:1943-8141/AJTR0146445

Original Article

TREM2 as an independent predictor of poor prognosis promotes the migration via the PI3K/AKT axis in prostate cancer

Hai-Tao Gao[1*], Zhan Yang[1*], Hao Sun[1], Yong Zhang[2], Zhu Wang[1], Wu-Yao Liu[1], Hong-Zhuang Wen[1], Chang-Bao Qu[1*], Xiao-Lu Wang[1*]

[1]Department of Urology, The Second Hospital of Hebei Medical University, Shijiazhuang, Hebei, China; [2]Department of Urology, National Cancer Center, Chinese Academy of Medical Sciences and Peking Union Medical College, Beijing, China. [*]Equal contributors.

Received September 12, 2022; Accepted December 30, 2022; Epub February 15, 2023; Published February 28, 2023

Abstract: Objective: Prostate adenocarcinoma (PRAD) is one of the most common cancers, with high morbidity and mortality. Triggering receptors expressed on myeloid cells 2 (TREM2) is upregulated in various malignancies, however its effect on PRAD remains unknown. This study aimed to investigate the prognostic value of TREM2 in PRAD. Methods: PRAD samples were collected from The Cancer Genome Atlas (TCGA), the Gene Expression Omnibus (GEO), Oncomine, and the Human Protein Atlas (HPA) to analyze the differences in TREM2 expression between normal and tumor tissues. The influence of TREM2 on the clinicopathological characteristics and its prognostic value were evaluated using the Kaplan-Meier curve, Cox regression analysis, ROC (receiver operating characteristic) plot, and nomogram. Gene Ontology (GO), gene set enrichment analysis (GSEA), and protein-protein interaction (PPI) were conducted to screen biological functions and pathways. The relationship between TREM2 and tumor microenvironment (TME) characteristics was explored. The TREM2 expression in PRAD specimens and cell lines was assessed by immunohistochemistry staining and western blot. TREM2-specific siRNAs were used to evaluate the effects of TREM2 on cell function. Results: TREM2 was upregulated and positively associated with poor clinicopathologic characteristics. Overexpression of TREM2 is an independent biomarker for the prognosis of PFI (progression-free interval). Moreover, TREM2 expression was positively correlated with various TME characteristics. Knockdown of TREM2 inhibited the migration of PRAD cell lines via the PI3K/AKT axis. Conclusion: High TREM2 expression may represent a novel diagnostic and prognostic biomarker and serve as a potential target gene for PRAD therapy.

Keywords: Bioinformatics, immune infiltrate, prognosis biomarker, prostate adenocarcinoma, TREM2

Introduction

Prostate cancer (PCa), namely prostate adenocarcinoma (PRAD), is the second major cause of cancer-associated death among men in the Western countries [1, 2]. According to the available data, PCa remains the main health risk among men, with an estimated 191,930 new cases and 33,330 PCa-related deaths in 2020 in the United States [3]. Although clinicians have used prostate-specific antigen (PSA), Gleason score, and other pathological makers to facilitate the early screening of PCa and estimate the prognosis after treatment, its morbidity and mortality are still extremely high because of the lack of reliable and effective biomarkers and therapeutic approaches for PCa. Additionally, there is considerable evidence suggesting that PCa is highly heterogeneous [4]. Therefore, personalized management represents a promising strategy for correcting the associated diagnosis and treatment defects. Consequently, further identification of specific biomarkers for the early detection of PCa is needed to improve diagnostic accuracy, assess treatment response, and explore new therapeutic targets [5].

The tumor microenvironment (TME) comprises a dynamic, interconnected network of malignant cells, tumor-infiltrating immune cells (TIICs), and stromal cells, as well as insoluble

factors such as chemokines and cytokines [6]. Within the TME infrastructure, the recruitment of immune and nonimmune cell types, as well as their secreted factors, is the potential driving force behind the development of chronic inflammatory and immunosuppressive state [7]. Malignant cells elicit multiple mechanisms of immunosuppression to counteract eradication by host immunosurveillance [8, 9]. Patients with metastatic PCa show disrupted cellular immunity, with a largely immunosuppressed TME [10, 11]. Immunotherapy is one approach having the potential to revolutionize the treatment of various tumors [12]. It exploits the ability of the immune system to target and kill carcinoma cells. Unfortunately, the clinical efficacy of immunotherapy is limited to varying degrees due to immunosuppressive TME and tumor-mediated immune escape mechanisms [9]. As such, elucidating the molecular mechanisms of tumor immunity will not only further enhance our understanding of how the TME regulates cancer but also provide novel immunotherapy targets for PRAD.

Triggering receptors expressed on myeloid cells 2 (TREM2), which was first identified as a novel activating receptor superfamily with a V-type extracellular domain [13], expresses mainly in dendritic cells (DCs) [14]. It is also found in nuclear cells [15], osteoclasts [16], macrophages [17], and microglia [18]. TREM2 depends on binding to the DNAX-activating protein 12 cytosolic linker to exert a pivotal function in regulating the secretion of proinflammatory cytokines and suppressing inflammation [15]. Recently, increasing evidence has illustrated that the aberrant TREM2 expression is significantly related to multiple malignancies, including renal cell carcinoma [19], gastric cancer [20, 21], and gliomas [22, 23], indicating that TREM2 can function as a prognostic marker due to its unique role in tumorigenesis. Importantly, TREM2, as an immunosuppressive receptor in modulating the TME [24], can stimulate suppressive cells such as myeloid-derived suppressor cells and tumor-associated macrophages (TAMs) [25, 26], while also curbing the antitumor immune response [27]. Therefore, reprogramming the TREM2 signaling pathway in the TME is essential to achieve a stronger antitumor effect.

Despite growing evidence of an association between TREM2 and various tumors, the underlying mechanisms by which TREM2 is regulated in PCa remain unclear. Therefore, the role of TREM2-mediated immune regulation should be elucidated through further studies. This study used integrated bioinformatics approaches and *in vitro* experiments to analyze the TREM2 expression in PRAD tissues and cell lines. Moreover, we used the tumor-immune system interactions and drugbank (TISIDB) database combined with the Tumor Immunity Estimation Resource (TIMER) database to explore the effect of TREM2 on TIIC and immune marker sets in PRAD. We also studied the potential mechanism underlying the regulation of TREM2 in PRAD.

Materials and methods

Data sources

We obtained the pan-cancer RNA-sequencing (RNA-seq) data from the Genotype-Tissue Expression (GTEx) portal and The Cancer Genome Atlas (TCGA) via the University of California Sata Cruz Xena (https://xenabrowser.net/datapages/) and processed them uniformly. The source of PRAD RNA-seq raw counts (tumor = 499, normal = 52) and relevant clinical data was TCGA (https://portal.gdc.cancer.gov/). The data downloaded from the database were in units of three high-throughput sequencing (HTSeq) fragments per kilobase, which were converted into transcripts per million for performing subsequent analysis. This study evaluated the TREM2 expression using the Oncomine database, Gene Expression Omnibus (GEO) database and the Human Protein Atlas (HPA) database.

Survival analysis

The association of TREM2 expression with disease prognosis was examined using a one-way Cox assessment method. This study also used Kaplan-Meier (KM) approach to analyze the relation of differential TREM2 expression with disease prognosis. Hence, we classified TREM2 expression in carcinoma and noncarcinoma samples as high and low TREM2 expression. One-way Cox survival results were visualized using the R package “Forest plot” with the survival software.

Gene ontology enrichment analysis

The differentially expressed genes (DEGs) related to TREM2 from TCGA were extracted to

acquire the gene expression pattern in PRAD. The thresholds used in the feature enrichment analysis were |logFC| > 1.0 and P_{adj} < 0.05. The Gene Ontology (GO) analysis comprising biological processes, molecular functionality, and cellular composition [28] was performed in this study using the clusterProfiler package in the statistical software R. A *P* value of < 0.05 indicated a statistically significant difference.

Protein-protein interaction network (PPI) analysis

The software Cytoscape (version 3.7.1) was applied to map the protein-protein interaction network of TREM2-related DEGs extracted from the STRING (Search Tool for the Retrieval of Interaction Gene/Proteins) database (http://string-db.org) (interaction score > 0.4) [29].

Gene set enrichment analysis

The underlying mechanisms of TREM2-related functionalities and pathways were elucidated in this study using clusterProfiler [30]. The enrichment of gene sets was considered significant when the normalized enrichment score was ≥ 1.0, the false discovery rate (FDR) was < 0.25, and the adjusted *P* was < 0.25.

Statistical analysis

The statistical analyses were carried out using the statistical software R ver. 3.6.3. In this study, the TREM2 gene expression was compared using the independent- and paired-sample *t* tests in the unpaired and paired samples, respectively. We assessed the correlation between the TREM2 expression and the clinicopathological features of PRAD based on the Wilcoxon rank-sum test combined with the independent-samples *t* test. The log-rank test was performed on the data in this study using the KM plot to explore the correlation between the TREM2 gene and progression-free interval (PFI) among the patients with PRAD. The receiver operating characteristic (ROC) and time-dependent curves were created using the pROC package to assess the diagnostic value of the TREM2 gene, wherein the specificity and accuracy of the ROC curves were predicted using the area under the curve (AUC). Moreover, we evaluated how the TREM2 expression impacted the PFI and other clinical characteristics using the single- and multi-variable Cox models. The R package regression modeling strategies (rms) and survival package were used to create the calibration plots and nomograms. A *P* value of < 0.05 indicated a statistically significant difference.

Collection of PRAD specimens and ethics statement

In this study, we collected 40 pairs of sample tissues from patients with PRAD who had undergone surgical resection between May 2020 and December 2021 at the Urology Department of the Hebei Medical University Second Hospital. The research protocol was approved by the ethics committee of the aforementioned hospital, and informed consent was acquired from all patients before participation in this study.

Immunohistochemistry (IHC) staining

This study assessed the TREM2 protein expression in 40 pairs of carcinoma and normal paracarcinoma tissues using IHC staining. Briefly, the tissue samples were immobilized in 10% formalin for 48 h, and the soaked tissue samples were embedded in paraffin. Then, the resulting samples were cut into 4-μm-thick slices for IHC staining using the Histostain-Plus kit (SP-9000, Zsgb Bio, China) following the manufacturer's protocols. Xylene was used to deparaffinize these sections, and gradient concentrations of ethanol were used for their rehydration. 3% H_2O_2 was used to quench the activity of endogenous peroxidase. Then, 0.1% trypsin was used to retrieve the antigens, and normal goat serum was used for 30 min of blockage. Following overnight incubation with anti-TREM2 primary antibody (13483-1-AP, 1:200 dilution; Proteintech) at 4°C, the sections were incubated with anti-rabbit immunoglobulin G polymer (enzyme-labeled) at 25°C for further 30 min. Thereafter, the chips were rinsed in phosphate-buffered saline (PBS) and incubated in diaminobenzidine for 5 min before immunostaining. The chip was then washed, dehydrated with alcohol and xylene, and mounted with a permanent medium. We examined the prepared chips under a microscope (Olympus, BX43). Two pathologists, who were blinded to the clinical data, evaluated the IHC scores independently. The intensity of staining was scored as 0, 1, 2, and 3, suggesting negative, weak, moderate, and strong interactions, separately. The posi-

tively stained cell ratio was scored as 0, 1, 2, 3, or 4, which indicated < 1%, 1-25%, 26-50%, 51-75%, and 76-100%, respectively. The number of positively stained cells *P* (0-4) was multiplied by the intensity of staining *I* (0-3). The values ranged from 0 to 12.

Cell culture and transfection

The human benign prostatic hyperplasia 1 (BPH-1) and PCa (PC-3, C4-2) cells used in this study were acquired from the American Type Culture Collection (VA, USA). The Roswell Park Memorial Institute 1640 medium (Gibco, MD, USA), containing 10% FBS (Gemini Foundation, USA), 100 μg/mL streptomycin, and 100 U/mL penicillin, was used for cellular growth and maintenance. The cells were cultured at 37°C in a humidified atmosphere with 5% CO_2. The TREM2-targeting small interfering RNA (si-RNA) and the corresponding negative control were obtained from GenePharma (Shanghai, China). The PC-3 and C4-2 cells were transfected based on Lipofectamine 2000 (Invitrogen) following the manufacturer's protocols, and the cells were harvested and lysed for Western blotting.

Transwell invasion assay

In this study, the cellular invasive potential was assessed using a 24-well Transwell chamber (Millipore, MA, USA), in which the pore size of the membrane was 8 μm. Matrigel (BD Biosciences, NJ, USA) was used to coat the upper membrane surface. In the upper chamber, a serum-free medium was used to resuspend the PC-3 and C4-2 cells (1×10^5 cells/well) to facilitate up to 36 h of cellular migration toward the lower chamber, which was filled with 10% fetal bovine serum (FBS). The chambers were subjected sequentially to washing with PBS twice, immobilization with 4% paraformaldehyde for 15 min, and staining using 0.1% crystal violet for 10 min. Then, the noninvasive cells on the upper membrane were removed using cotton swabs. Finally, the numbers of invasive cells in 10 random fields were determined on each membrane under an Olympus BX43 microscope.

Wound healing assay

In this study, the migratory capacity of the cells was determined using the wound healing assay. Briefly, after plating onto six-well microplates, the PC-3 and C4-2 cells were grown to 70% confluence. Then, the adherent monolayer of cells was scraped using a sterilized pipette tip. The PBS tablets were rinsed twice to remove the floating cells, and a fresh medium was supplemented. After 36 h of further preparation, the number of transferred cells was counted with an inverted microscope (CKX41; Olympus, Tokyo, Japan).

Quantitative real-time polymerase chain reaction

The TRIzol reagent (Invitrogen, CA, USA) was used to extract total RNAs from the PC-3, C4-2, and BPH-1 cells, which were then reverse-transcribed into complementary DNA using the PrimeScript reverse transcription kit (TaKaRa) following the manufacturer's protocol. Then, quantitative real-time polymerase chain reaction was performed using the SYBR Green assay (V azyme) on the StepOnePlus system (Life Technologies, CA, USA). The primer sequences of TREM2 were as follows: forward, 5'-GGAGCACAGCCATCACAGAC-3'; reverse, 5'-CACATGGGCATCCTCGAAGC-3'. GAPDH was applied as the internal control. The expression levels were estimated using relative $2^{-\Delta\Delta Ct}$ quantification.

Western blotting

After washing with PBS, the cells were placed in a mixture containing the protease inhibitor (Sigma-Aldrich) at 4°C for 20 min. The Coomassie protein assay reagent (Pierce) was used for determining the total protein concentration in cellular lysates. Aliquots of the proteins were isolated on SDS-PAGE gels (10%) and then electro-transferred onto polyvinylidene fluoride membranes (Millipore). Next, the membranes were blocked for 2 h in TTBS using skimmed milk (5%) at ambient temperature, following which overnight probing was performed at 4°C using the designated primary antibodies such as anti-TREM2 (13483-1-AP, 1:1000 dilution; Proteintech, IL, USA), anti-matrix metallopeptidase (MMP)-9 (10375-2-AP, 1:500; Proteintech), anti-vimentin (10366-1-AP, 1:1000; Proteintech), anti-β-catenin (51067-2-AP, 1:1000; Proteintech), anti-PD-L1 (66248-1-Ig, 1:1000; Proteintech), anti-p-Akt (66444-1-Ig, 1:1000; Proteintech), anti-Akt (10176-2-AP, 1:1000; Proteintech), anti-p-phosphoinositide 3-kinases (PI3K) (ab182651, 1:500; Proteintech), anti-PI3K (20584-1-AP, 1:1000; Protein-

Table 1. The clinical features of PRAD patients

Characteristic	levels	Overall
n		499
T stage, n (%)	T2	189 (38.4%)
	T3	292 (59.3%)
	T4	11 (2.2%)
N stage, n (%)	N0	347 (81.5%)
	N1	79 (18.5%)
M stage, n (%)	M0	455 (99.3%)
	M1	3 (0.7%)
Primary therapy outcome, n (%)	PD	28 (6.4%)
	SD	29 (6.6%)
	PR	40 (9.1%)
	CR	341 (77.9%)
Race, n (%)	Asian	12 (2.5%)
	Black or African American	57 (11.8%)
	White	415 (85.7%)
Age, n (%)	≤ 60	224 (44.9%)
	> 60	275 (55.1%)
Residual tumor, n (%)	R0	315 (67.3%)
	R1	148 (31.6%)
	R2	5 (1.1%)
Zone of origin, n (%)	Central Zone	4 (1.5%)
	Overlapping/Multiple Zones	126 (45.8%)
	Peripheral Zone	137 (49.8%)
	Transition Zone	8 (2.9%)
PSA (ng/ml), n (%)	< 4	415 (93.9%)
	≥ 4	27 (6.1%)
Gleason score, n (%)	6	46 (9.2%)
	7	247 (49.5%)
	8	64 (12.8%)
	9	138 (27.7%)
	10	4 (0.8%)
PFI event, n (%)	Alive	405 (81.2%)
	Dead	94 (18.8%)

CR, complete response; PD, progressive disease; SD, stable disease; PR, partial response; PSA, prostate-specific antigen; PFI, progression-free interval.

tech), or anti-GAPDH (60004-1-Ig, 1:5000; Proteintech). Following incubation for 1 h using horseradish peroxidase-labeled secondary antibody (1:10,000, Rockland) at ambient temperature, the ECL system (Thermo Fisher Scientific, NY, USA) was applied for visualizing the blots.

Results

Baseline characteristics of patients with PRAD

The RNA-seq data and clinical characteristics of 499 patients were acquired based on TCGA. The detailed clinical characteristics, including age, ethnicity, T, N, and M stages, Gleason score, primary prognosis, tumor residue, region of origin, PSA, and PFI, are presented in **Table 1**.

TREM2 upregulation in patients with different cancers and PRAD

To identify the status of TREM2 expression in multiple tumors, we first analyzed the transcription levels of TREM2 based on TCGA database. The TREM2 mRNA expression was upregulated in nearly all tumor types, including invasive breast cancer, bladder urothelial carcinoma, cervical squamous cell carcinoma, endocervical adenocarcinoma, esophageal cancer, cholangiocarcinoma, colon adenocarcinoma, head and neck squamous cell carcinoma, glioblastoma multiforme, hepatocellular carcinoma, renal papillary cell carcinoma, rectal adenocarcinoma, renal clear cell carcinoma, gastric adenocarcinoma, pulmonary adenocarcinoma, and uterine corpus endometrial carcinoma ($P < 0.001$; **Figure 1A**). The expression patterns of TREM2 mRNA were predicted using the TCGA to further determine the significance of the TREM2 expression in patients with PRAD. A markedly elevated mRNA level of TREM2 was observed in the PRAD tissues compared with the normal prostate tissues (**Figure 1B**). We also examined the TREM2 mRNA expression in PRAD tissues and corresponding para-carcinoma tissues in the TCGA dataset, and verified that TREM2 was highly expressed in tumor tissues ($P < 0.05$; **Figure 1C**). Consistent with the above findings, the expression of TREM2 was elevated relative to normal tissue controls from the Oncomine and GEO databases (dataset GSE46602) ($P < 0.001$; **Figure 1D**, **1E**). Finally,

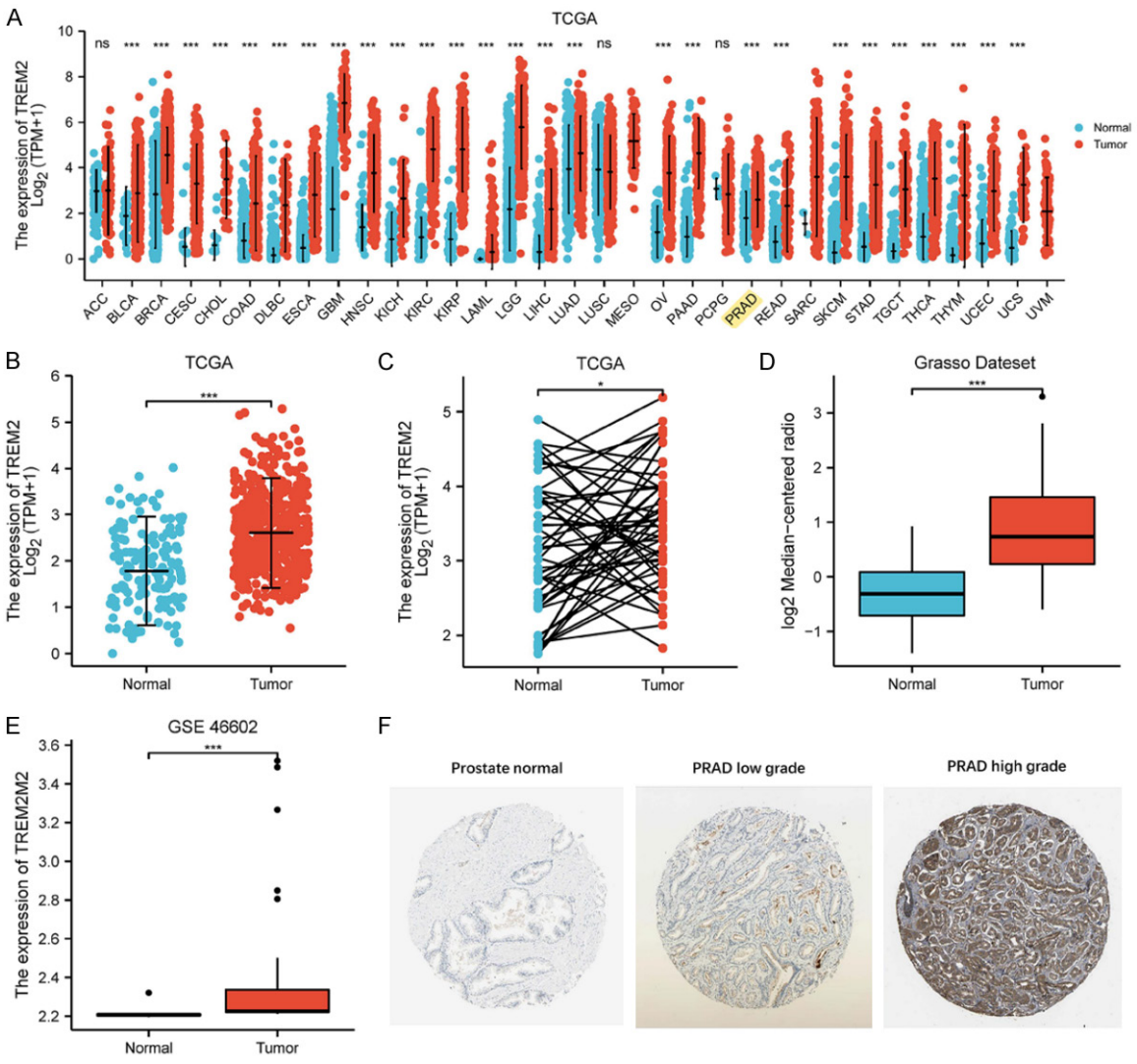

Figure 1. TREM2 expression in patients with PRAD. A. TREM2 mRNA expression in various human carcinomas in the TCGA database; B. TREM2 mRNA expression in PRAD and normal samples in the TCGA database; C. TREM2 mRNA expression in PRAD and normal samples, as well as in matched adjacent samples in the TCGA database; D. TREM2 mRNA expression in PRAD and normal samples in the Oncomine data set; E. TREM2 mRNA expression in PRAD and normal samples in the GSE46602 data set; F. TREM2 protein expressions in PRAD and normal samples in the Human Protein Atlas ($^{*}P < 0.05$, $^{***}P < 0.001$).

we also investigated the protein expression patterns according to the Human Protein Atlas (HPA). Significant TREM2 upregulation was observed in patients with PRAD ($P < 0.001$; **Figure 1F**). These results indicate that TREM2 may facilitate prostate carcinogenesis.

Relationship between TREM2 upregulation and poor clinicopathological characteristics in patients with PRAD

To explore the relationship between TREM2 expression and clinicopathological characteristics of PRAD, 499 PCa samples were collected from TCGA database. The TREM2 upregulation showed a significant correlation with the clinical T ($P < 0.001$; **Figure 2A**), N ($P < 0.001$; **Figure 2B**), and M stages ($P < 0.05$; **Figure 2C**), Gleason score ($P < 0.001$; **Figure 2D**), primary treatment outcome ($P < 0.001$; **Figure 2E**), residual tumor ($P < 0.001$; **Figure 2F**), age ($P < 0.001$; **Figure 2G**), and PFI ($P < 0.001$; **Figure 2H**). Therefore, an increase in TREM2 expression was probably linked to poorer clinicopathological features and more aggressive behavior in PRAD.

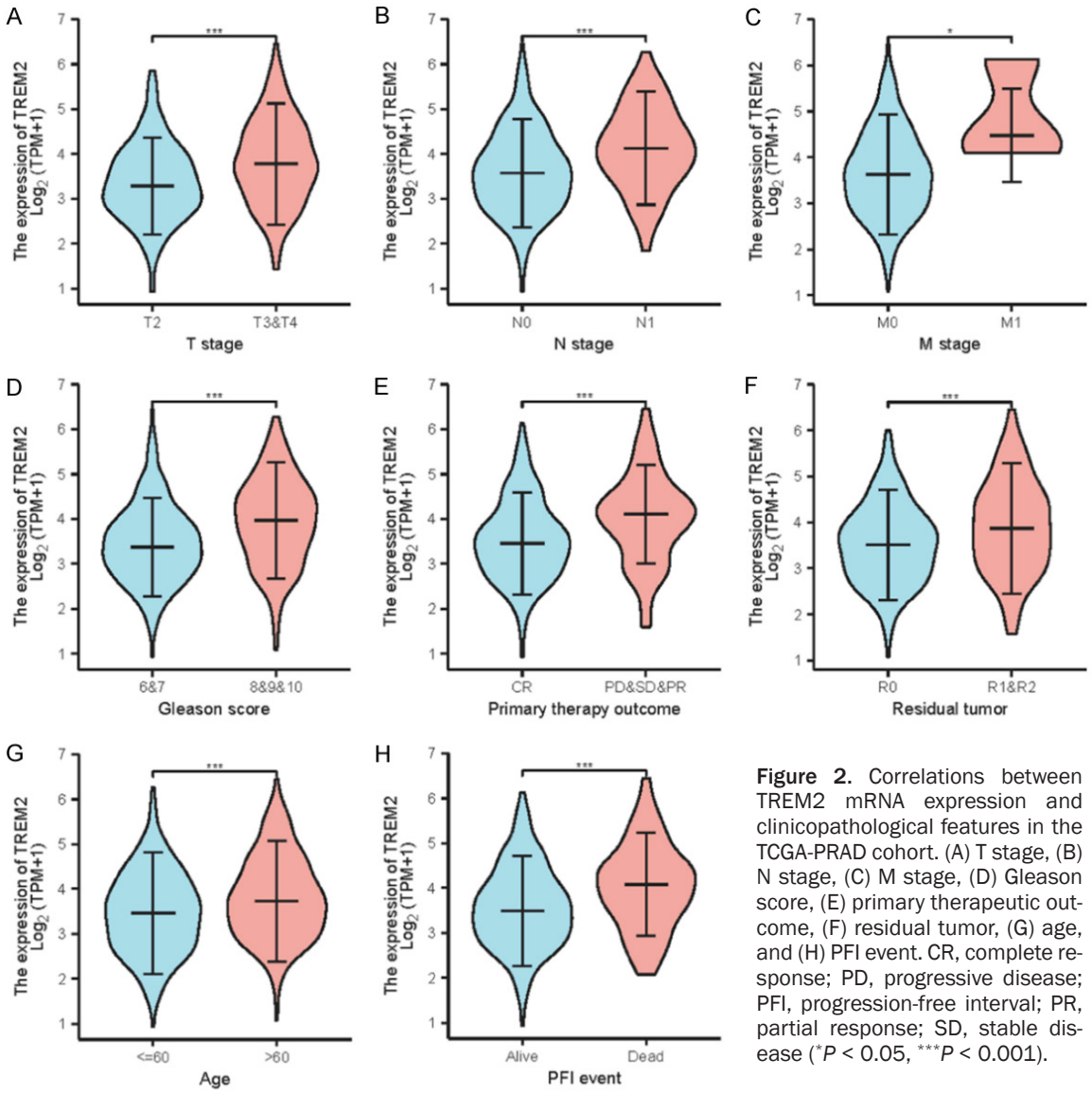

Figure 2. Correlations between TREM2 mRNA expression and clinicopathological features in the TCGA-PRAD cohort. (A) T stage, (B) N stage, (C) M stage, (D) Gleason score, (E) primary therapeutic outcome, (F) residual tumor, (G) age, and (H) PFI event. CR, complete response; PD, progressive disease; PFI, progression-free interval; PR, partial response; SD, stable disease ($^{*}P < 0.05$, $^{***}P < 0.001$).

TREM2 upregulation: an independent prognostic factor in patients with PRAD

Next, we explored whether TREM2 served as an independent factor for the prognosis of patients with PRAD. The KM survival assessment (**Figure 3A**) revealed that the TREM2 upregulation in patients with PRAD was linked to shorter PFI, with a hazard ratio (HR) of 2.04 and a confidence interval (CI) of 1.32-3.13 ($P = 0.001$). In the clinical T stage (HR = 1.99, CI = 1.29-3.06, $P = 0.002$; Figure S1A), N stage (HR = 2.03, CI = 1.29; Figure S1B), M stage (HR = 2.06, CI = 1.33-3.20, $P = 0.001$; Figure S1C), PSA (HR = 2.09, CI = 1.34-3.26, $P = 0.001$; Figure S1D), Gleason score (HR = 1.63, CI = 1.00-2.63, $P = 0.048$; Figure S1E), and residual tumor (HR = 2.00, CI = 1.29-3.09, $P = 0.002$; Figure S1F), the subgroups with high TREM2 expression had worse PFI. We used the ROC curve to demonstrate the diagnostic value of TREM2 expression (**Figure 3B**) and observed that TREM2 expression exhibited significantly high specificity and sensitivity (AUC = 0.746) for the diagnosis of PRAD. We predicted the 1-, 3-, and 5-year PFIs by creating the time-dependent survival ROC curves of TREM2 (**Figure 3C**), with AUCs of 0.667, 0.645, and 0.613, respectively, indicating that TREM2 was a suitable predictive marker. Furthermore, we performed a Cox regression analysis of representative clinical outcomes. It was observed that the TREM2 level

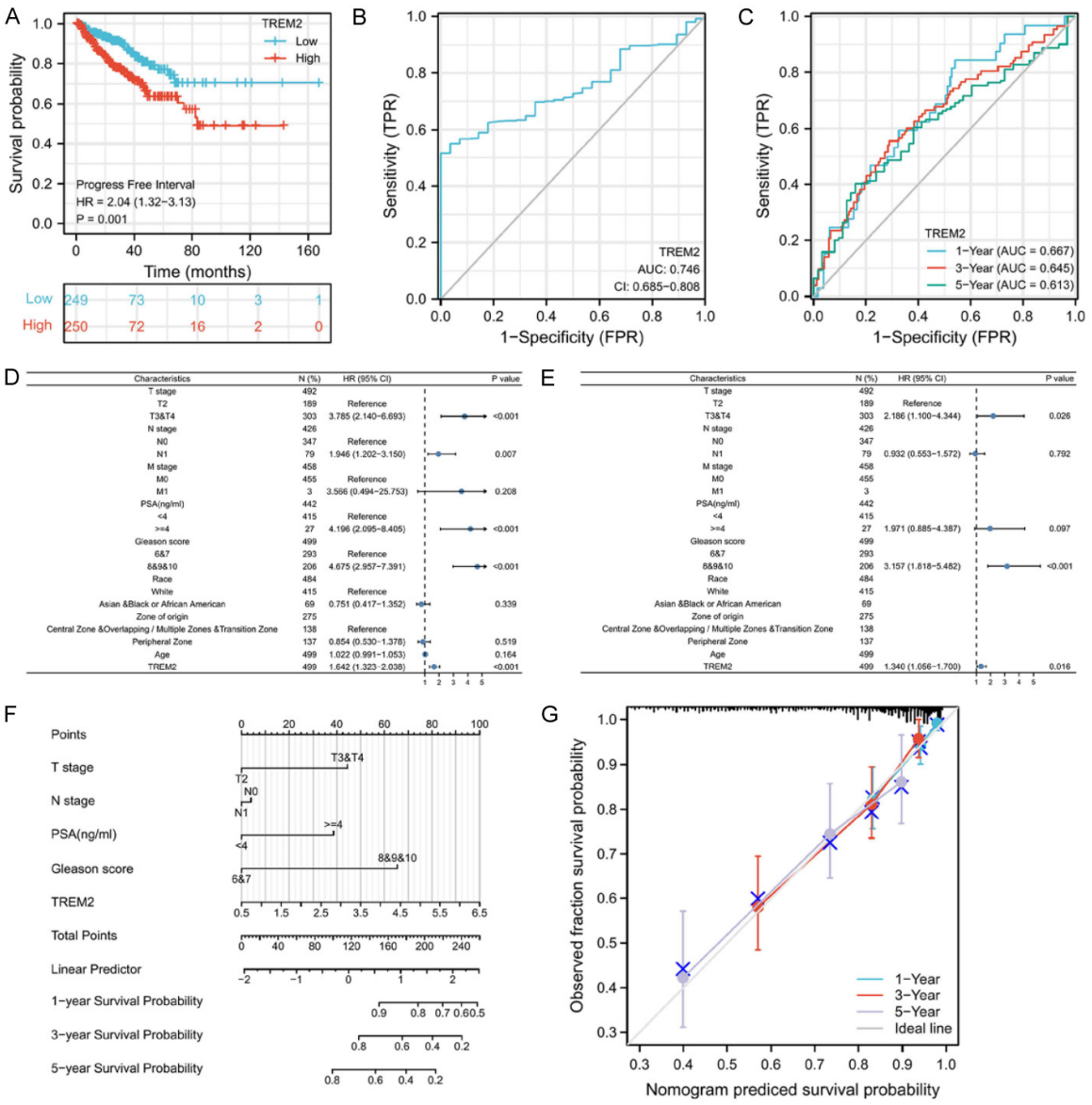

Figure 3. Diagnostic value of TREM2 expression in PRAD from the TCGA database. A. KM assessments for the correlation of TREM2 expression level with PFI. B. ROC plots for TREM2 in PRAD, healthy, and matched para-carcinoma samples. C. ROC plots against time at 1-, 3-, and 5-year PFIs. D and E. Associations of the TREM2 expression and other clinicopathological features with PFI among the patients with PRAD based on the single- and multi-variable Cox assessments. F. Probability forecasting nomograms at 1-, 3-, and 5-year PFIs in patients. G. Calibration curve of the nomogram for predicting PFI after 1, 3, and 5 years.

was an independent risk factor for PFI, with an HR of 1.340 and a CI of 1.056-1.700 (P = 0.016) in both univariate and multivariate Cox regression analyses (**Figure 3D**, **3E**). Based on the multivariate Cox analysis, the 1-, 3-, and 5-year PFIs of the patients were predicted by incorporating the clinical T and N stages, PSA, Gleason score, and TREM2 into the nomogram with a C-index of 0.732 (**Figure 3F**). The efficiency of the nomogram was examined using the calibration curve (**Figure 3G**), revealing the consistency between the actual and predicted survival probabilities. Therefore, the TREM2 upregulation was an independent marker of PFI prognosis in patients with PRAD.

Constructing protein-protein interaction networks and functional annotation of genes associated with TREM2 in patients with PRAD

We first divided the PRAD samples into high- and low-expression groups depending on the

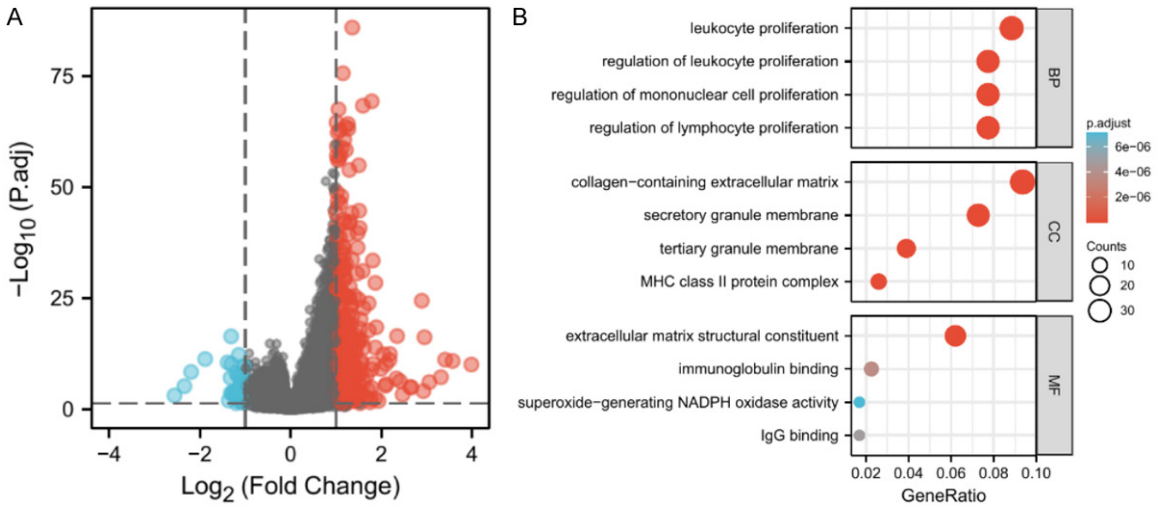

Figure 4. PPI network and assessment of TREM2 gene enrichment in PRAD. A. Volcano plot illustrating the DEGs between the groups with TREM2 downregulation and upregulation. B. GO term analyses for genes associated with TREM2.

median TREM2 mRNA expression in the TCGA database (|logFC| > 1.0, adjusted *P* value < 0.05) to effectively evaluate the biological functions of TREM2-related DEGs. The volcano plot demonstrated 732 DEGs, among which 557 were upregulated and 175 downregulated (**Figure 4A**) ($P < 0.01$). Then, we used the clusterProfiler package to analyze GO function enrichment. The results confirmed the association of TREM2 co-expressing genes with the regulation of leukocyte proliferation, monocytes and lymphocytes (**Figure 4B**). We performed a PPI analysis using the STRING online database to further explore the interaction of differentially expressed TREM2 in PRAD and screened out the 30 most important genes using the Cytoscape software (Figure S2).

TREM2-associated signaling pathway enrichment analysis based on gene set enrichment analysis

It is of critical importance to elucidate the mechanism of TREM2-associated signaling pathways governing its activity and regulation in the progression of PRAD. Therefore, the gene set enrichment analysis (GSEA) dataset with high TREM2 expression differed significantly from that with low expression based on the MsigDB collection (c2.cp.v7.2.2) (adjusted $P < 0.05$; FDR < 0.05). Significant enrichments of the PI3 K/Akt axis and cancer pathways were observed in the group with high TREM2 expression (**Figure 5A**, **5B**). Several immune-related signaling pathways were significantly associated with the TREM2 overexpression, including cytokine-cytokine receptor interactions, cytokines, inflammatory responses, B cell receptor signaling, and chemotaxis factor signaling pathway (**Figure 5C-F**).

Analysis of the association between the TREM2 expression and the TME in patients with PRAD

TME has now been recognized to induce a critical function in regulating the progression of carcinoma, while TIIC is an independent factor in predicting the sentinel node status or survival among patients with cancer [31, 32]. Considering these key roles, we investigated the association of TREM2 with the immune infiltration in PRAD acquired from the TIMER database [33]. The results demonstrated that the TREM2 level was negatively associated with the purity of the tumor ($r = -0.16$) and positively related to the infiltration level of B cells ($r = -0.273$), $CD8^+$ T cells ($r = 0.069$), $CD4^+$ T cells ($r = 0.344$), macrophages ($r = 0.323$), neutrophils ($r = 0.281$), and dendritic cells (DCs) ($r = 0.433$) (**Figure 6A**). Moreover, we investigated the immune infiltration at different levels of TREM2 expression in PRAD based on the single-sample GSEA (ssGSEA) algorithm and confirmed that the TREM2 upregulation in the patients with PRAD was related to markedly higher infil-

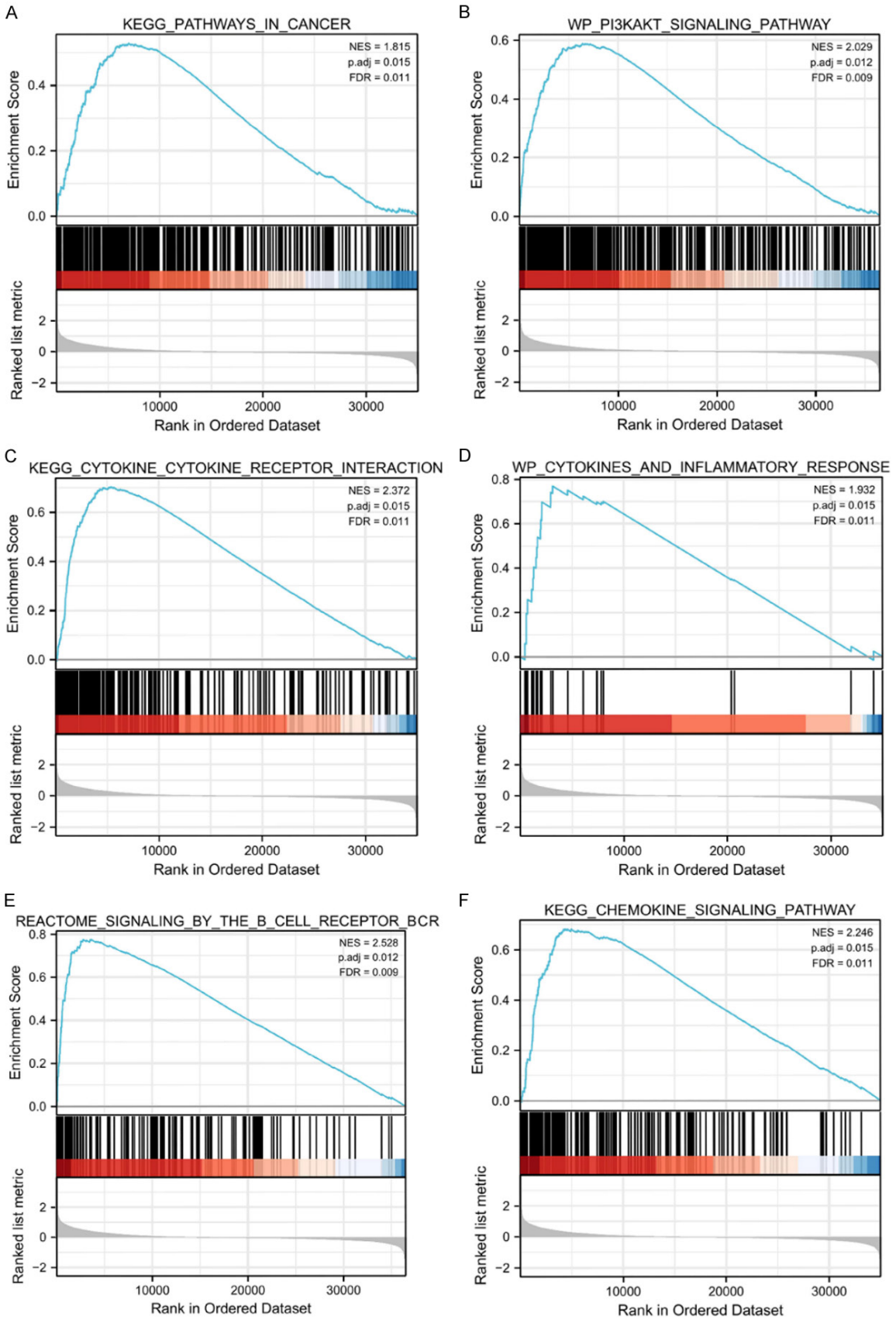
A
KEGG_PATHWAYS_IN_CANCER
NES = 1.815
p.adj = 0.015
FDR = 0.011
B
WP_PI3KAKT_SIGNALING_PATHWAY
NES = 2.029
p.adj = 0.012
FDR = 0.009
C
KEGG_CYTOKINE_CYTOKINE_RECEPTOR_INTERACTION
NES = 2.372
p.adj = 0.015
FDR = 0.011
D
WP_CYTOKINES_AND_INFLAMMATORY_RESPONSE
NES = 1.932
p.adj = 0.015
FDR = 0.011
E
REACTOME_SIGNALING_BY_THE_B_CELL_RECEPTOR_BCR
NES = 2.528
p.adj = 0.012
FDR = 0.009
F
KEGG_CHEMOKINE_SIGNALING_PATHWAY
NES = 2.246
p.adj = 0.015
FDR = 0.011
Enrichment Score
Ranked list metric
Rank in Ordered Dataset
10000
20000
30000

Figure 5. Enrichment plots based on the GSEA. Differential enrichment of a few pathways was noted in PRAD according to TREM2 upregulation and downregulation. FDR, false discovery rate; NES, normalized enrichment score; P adj, adjusted *P* value.

tration levels of $CD8^+$ T, NK, B, and DCs, as well as macrophages, compared with that in the patients with low TREM2 expression (Figure S3A). We used the ssGSEA algorithm to further analyze the TREM2 correlation with the immune infiltration in PRAD, and found that the TREM2 expression showed a positive association with the infiltration levels of $CD8^+$ T cells ($r = 0.225$, $P < 0.001$), B cells ($r = 0.214$, $P < 0.001$), DCs ($r = 0.437$, $P < 0.001$), neutrophils ($r = 0.293$, $P < 0.001$), and macrophages ($r = 0.574$, $P < 0.001$) (**Figures 6B-D** and S3B, S3C). Then, we analyzed various immune cell markers using the TIMER database and observed the association of these markers with TREM2 expression in PRAD (**Table 2**).

Chemokines and their receptors are emerging as a critical regulators of the remodeling of the TME [34, 35]. Therefore, we further analyzed the association of the TREM2 expression with the chemokines and their receptors. As shown in Figure S3D & S3E, there were significant associations between multiple tumor cell-associated chemokine receptors and chemokines and the TREM2 expression, including CCL3 ($r = 0.437$, $P < 0.001$), CL17 ($r = 0.405$, $P < 0.001$), CCL18 ($r = 0.445$, $P < 0.001$), CCR2 ($r = 0.359$, $P < 0.001$), CCR5 ($r = 0.429$, $P < 0.001$), and CXCR4 ($r = 0.359$, $P < 0.001$) (**Figures 6E-J** and S3D, S3E).

The use of the Immune Score, Stromal Score and Estimate Score are possible strategies to assess and quantify immune and matrix components in PRAD [36]. Obviously, the TREM2 expression was closely related to the Estimated Score ($r = 0.590$), immune Score ($r = 0.540$), and stromal Score ($r = 0.530$) (**Figure 7A-C**).

Emerging evidence has indicated the critical role of immune checkpoints in tumor immune escape, which was also an important predictor of the immune checkpoint inhibitor (ICI) treatment effect. In the PRAD samples of the TCGA, TREM2 was positively associated with the levels of Programmed Death 1 (PD-1) ($r = 0.280$), Programmed Cell Death-Ligand 1 (PD-L1) ($r = 0.260$), and Cytotoxic T Lymphocyte-associated Protein 4 (CTLA4) ($r = 0.320$) (**Figure 7D-F**). Subsequently, the association between the presence of immunomodulators and the TREM2 level in pan-cancer was analyzed using the TISIDB database (**Figure 8A**). **Figure 8B-G** showed the highest correlation between TREM2 and the six immunomodulators in PRAD.

TREM2 upregulation in PRAD tissue and stable cell lines

To further validate the results of the HPA databases at the experimental level, we examined the TREM2 protein expression in 40 pairs of carcinoma and normal para-carcinoma tissues using IHC and Western blotting. Contrary to the para-carcinoma tissues, the PRAD tissues demonstrated a significantly elevated TREM2 protein level ($P < 0.001$) (**Figure 9A**, **9B**). However, although a high TREM2 level was linked to the Gleason score, it was not statistically significant (data not shown). Besides, the mRNA and protein levels of TREM2 in the PRAD cells were validated, revealing significantly elevated levels in the C4-2 and PC-3 cells compared with the BPH-1 cells (**Figure 9C**, **9D**).

TREM2 knockdown suppressed the migration and invasion of PRAD cell lines

The above studies verified a significant increase in TREM2 expression in PRAD, indicating that TREM2 could function as an oncogene. Therefore, we transfected the TREM2-siRNA into C4-2 and PC-3 cells to better evaluate the role of TREM2 in cell function. Clearly, compared with the controls, the TREM2 protein level was significantly downregulated following the treatment of TREM2-siRNA (**Figure 9G**). Subsequently, the wound healing and Transwell assays revealed that the TREM2 knockdown suppressed the invasive and migratory potentials of C4-2 and PC-3 cells after 36 h (**Figure 9E**, **9F**). Western blotting further demonstrated that the TREM2 knockdown inhibited the expression of epithelial-mesenchymal transition (EMT)-related proteins, such as β-catenin,

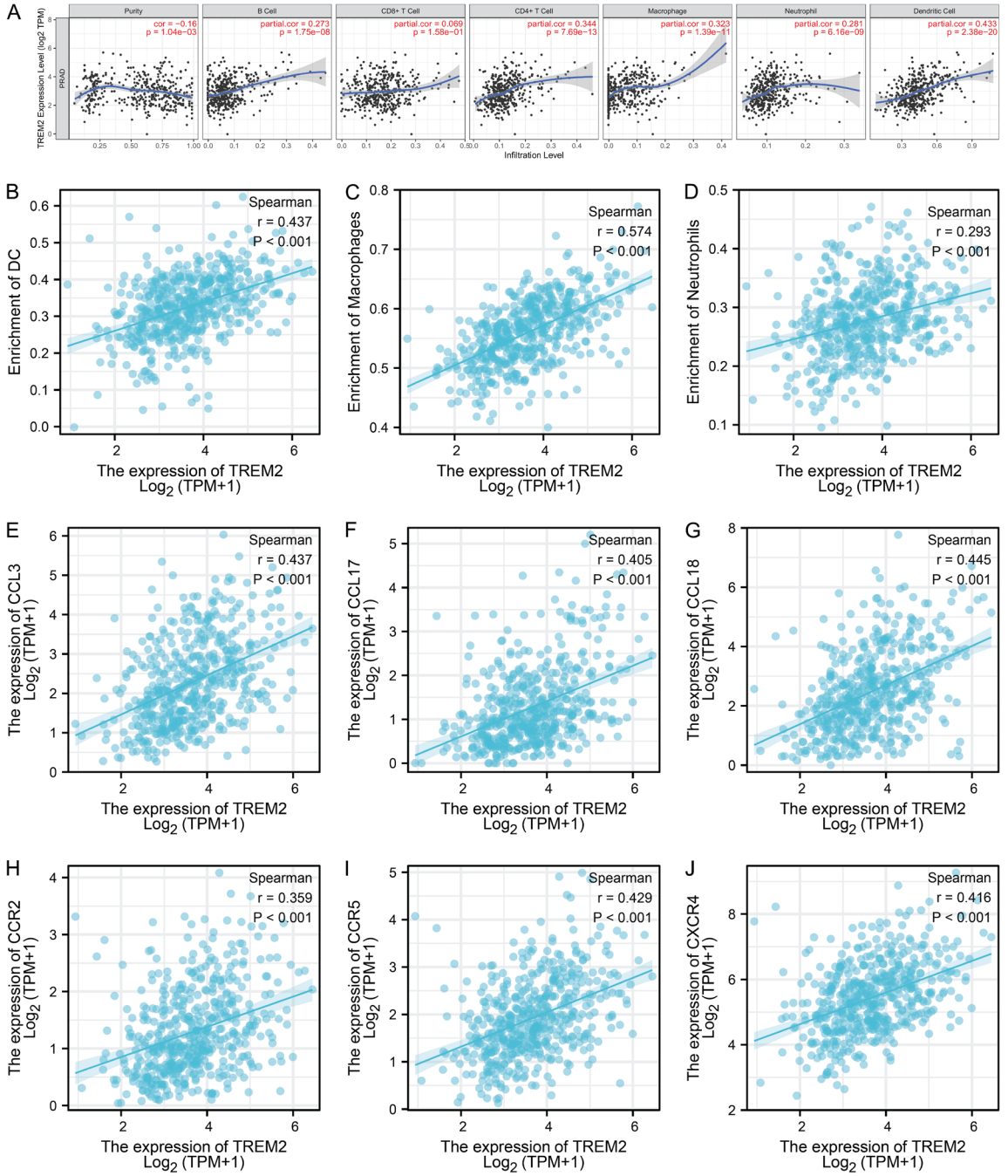

Figure 6. Association of TREM2 expression level with TIICs, chemokines and/or their receptors in PRAD. (A) Association of the TREM2 expression with the immune infiltration levels based on the TIMER database. (B-D) Association of the TREM2 expression with the immune infiltration in PRAD: (B) DCs; (C) macrophages; (D) neutrophils. (E-J) Associations of the TREM2 expression levels with chemokines and/or their receptors in PRAD: (E) CCL3, (F) CCL17, (G) CCL18, (H) CCR2, (I) CCR5, and (J) CXCR4. $^{***}P < 0.001$. C-C Motif Chemokine Ligand, CCL; C-C Motif Chemokine Receptor, CCR; C-X-C Motif Chemokine Receptor, CXCR.

MMP-9, and vimentin. More importantly, the PD-L1 expression decreased along with the lowered TREM2 protein levels (**Figure 9G**). Further studies demonstrated that TREM2 promoted the progression of PRAD via the PI3K/Akt pathway (**Figure 9H**).

Discussion

PCa remains the second major cause of cancer-associated deaths among men in western developed countries [1, 2]. Although serum PSA screening has been introduced to detect PCa in

Table 2. Correlation analysis between TREM2 and markers of immune cells in TIMER

Cell type	Gene maker	None		Purity	
		Cor	P	Cor	P
B cell	CD19	0.175	***	0.126	***
	CD38	-0.18	***	-0.23	***
Tfh	CXCR5	0.266	***	0.226	***
	ICOS	0.361	***	0.348	***
	BCL-6	0.034	***	-0.053	***
Th1	IL12RB2	0.218	***	0.203	***
	WSX-1	0.252	***	0.21	***
	T-BET	0.398	***	0.388	***
Th2	CCR3	0.26	***	0.262	***
	STAT6	0.006	***	-0.024	***
	GATA-3	0.181	***	0.159	***
Th9	TGFBR2	0.285	***	0.243	***
	IRF4	0.332	***	0.32	***
Th17	IL-23R	0.169	***	0.156	***
	IL-21R	0.397	***	0.385	***
	STAT3	0.031	***	-0.012	***
Th22	CCR10	0.287	***	0.24	***
	AHR	0.289	***	0.276	***
Treg	FOXP3	0.373	***	0.35	***
	CCR8	0.297	***	0.286	***
	CD25	0.414	***	0.39	***
T Cell exhaustion	PD-1	0.283	***	0.253	***
	CTLA4	0.343	***	0.321	***
Macrophage	CD68	0.762	***	0.763	***
	CD11b	0.531	***	0.524	***
M1	NOS2	0.077	***	0.035	***
	ROS	0.154	***	0.154	***
M2	ARG1	0.115	***	0.109	***
	MRC1	0.356	***	0.338	***
TAM	HLA-G	0.199	***	0.164	***
	CD80	0.431	***	0.415	***
	CD86	0.644	***	0.66	***
Monocyte	CD14	0.637	***	0.63	***
	CD16	0.673	***	0.667	***
NK	XCL1	0.325	***	0.302	***
	KIR3DL1	0.143	***	0.13	***
	CD7	0.345	***	0.323	***
Neutrophil	CD15	-0.035	***	-0.047	***
	MPO	0.235	***	0.186	***
DC	CD1C	0.301	***	0.3	***
	CD141	0.247	***	0.17	***

Th, T-helper type; Tregs, regulatory T cells; M, macrophage; TAM, tumor-associated macrophages; NK, natural killer cell; DC, dendritic cell.

an early stage, it has low sensitivity and specificity, which results from the considerable heterogeneity of PCa [4]. Therefore, further identification of specific early-detection biomarkers is urgently needed to improve the accuracy of the prediction of the invasiveness of PCa. In this study, using an integrated bioinformatics approach and *in vitro* experiments, we confirmed the significant TREM2 upregulation in PRAD tissues and cell lines, and its close association with adverse clinicopathological features. Based on the results of KM survival and multivariate Cox regression analysis, we predicted that TREM2 upregulation could lead to worse PFI in patients with PRAD, indicating its possible role as an independent biomarker for prognosis. Moreover, the TREM2 upregulation was positively linked to the immune infiltration levels of $CD8^+$ T, $CD4^+$ T, B cells, DCs, macrophages, and neutrophils. Furthermore, the TREM2 level was closely associated with diverse immune biomarkers in PRAD. Finally, the TREM2 knockdown significantly impaired the invasive and migratory potentials of PC-3 and C4-2 cells via the Akt/PI3K signaling pathway.

Recently, the critical effect of TREM2 on the progression of carcinoma and its possible role as a biomarker have attracted widespread attention [37]. TREM2 expression abnormalities have been observed in a series of malignant tumors, and its expression increases and functions to promote carcinogenesis in glioma [22], lung cancer [25], and gastric cancer [20]. Based on the TCGA, Oncomine, HPA, and Gene Expression Omnibus databases (data set GSE46602), our results showed that the mRNA level of TREM2 was upregulated in almost all tumor types compared with normal tissues, particularly PRAD. Nevertheless, TREM2 shows decreased expression in both colorectal cancer [38] and hepatocellular carcinoma [39], in which it demonstrates antitumor effects. This heterogeneity could be accounted for by tumor cell biodiversity. In this study, we observed that the TREM2 upregulation was related to worse clinicopathological features such as age, Gleason score, T, N, and M stages, primary prognosis, tumor residue, and PFI. Moreover, both KM survival and multi-variable Cox assessments revealed that TREM2 upregulation predicted the worse PFI in patients with PRAD, suggest-

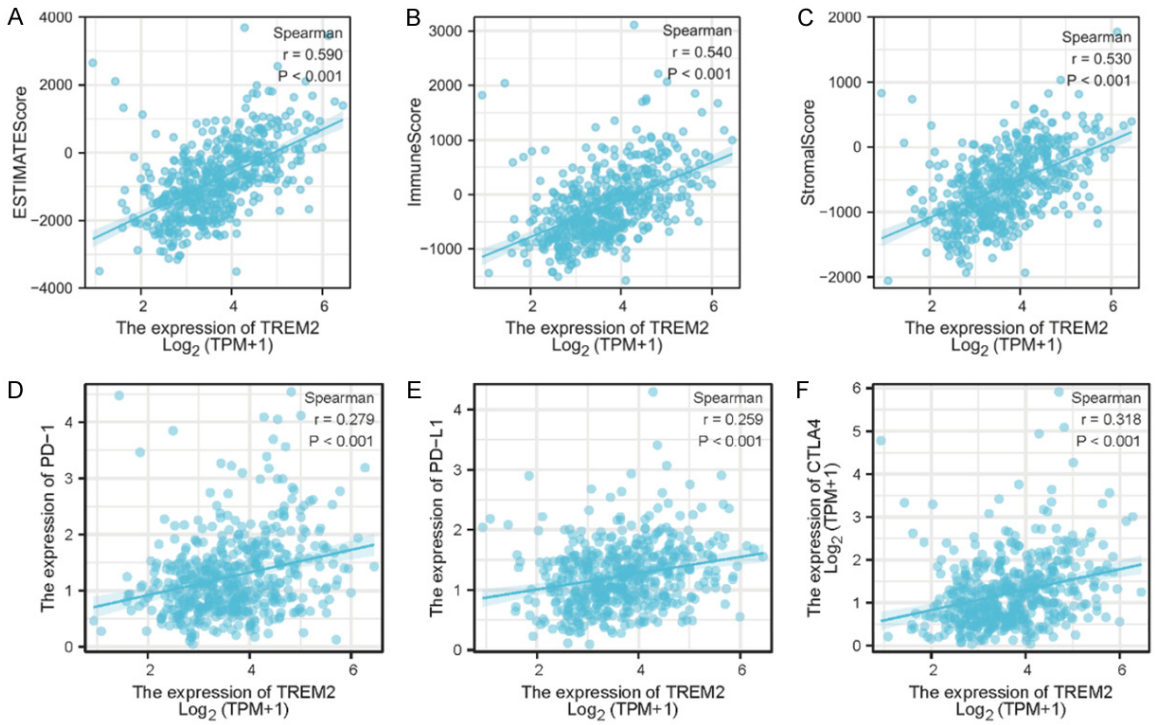

Figure 7. Correlations of the TREM2 expression levels with the stromal-immunity scores in PRAD. (A) Estimate score, (B) Immune score, (C) Stromal score, (D) PD-1, (E) PD-L1, and (F) CTLA4.

ing its value as an independent prognostic marker. Unfortunately, very few studies have unraveled the underlying biological mechanisms of TREM2 in PRAD.

Increasing evidence has revealed that TMEs can reprogram cancer biology in various aspects and have the potential as therapeutic targets, especially in immunotherapy. However, tumors often establish an immunosuppressive environment by recruiting tolerant immune cells and releasing immunosuppressive cytokines that promote immune tolerance and resistance to immunotherapy [9]. In terms of TREM2, current evidence demonstrates that TREM2 plays an essential role as a main pathologically induced immune signaling hub for remodeling the TME [27, 40]. Upregulation of TREM2 has been observed in peripheral blood mononuclear cells and TAMs isolated from patients with lung cancer and tumor-bearing mice compared to healthy controls. Moreover, $TREM2^+$ myeloid cells are effectively inhibitory to T cell proliferation in vitro, while the levels of $TREM2^+$ macrophages around tumor cells showed a positive correlation with tumor progression. As such, identification of TREM2 signaling pathways may reshape the TME and produce a robust antitumor effect. In this study, GO annotation and pathway enrichment analyses were carried out using the GSEA. The results confirmed the implication of the TREM2-related genes in regulating the proliferation of leukocytes, mainly monocytes, and lymphocytes. The GSEA also revealed a significant correlation of some immune-related signaling pathways with TREM2 upregulation. These included cytokine-cytokine receptor interactions, cytokines, inflammatory responses, B cell receptor signaling, and chemokine signaling.

TIIC, a prominent constituent of the TME, are thought to be a consequence of immunosuppression that contributes to neoplastic progression and poor prognosis, including PCa [41, 42]. The survival analysis suggests that high intra-tumoral infiltration of $CD4^+$ or $CD8^+$ lymphocytes predicts not only worse biochemical failure-free survival but also PCa-specific survival [43-45]. TAMs are recruited into the TME via CCL2-CCR2 signaling, and their presence is associated with poorer prognosis and higher Gleason scores [46, 47]. Moreover, M2 $CD68^+$ macrophages favor the progression of

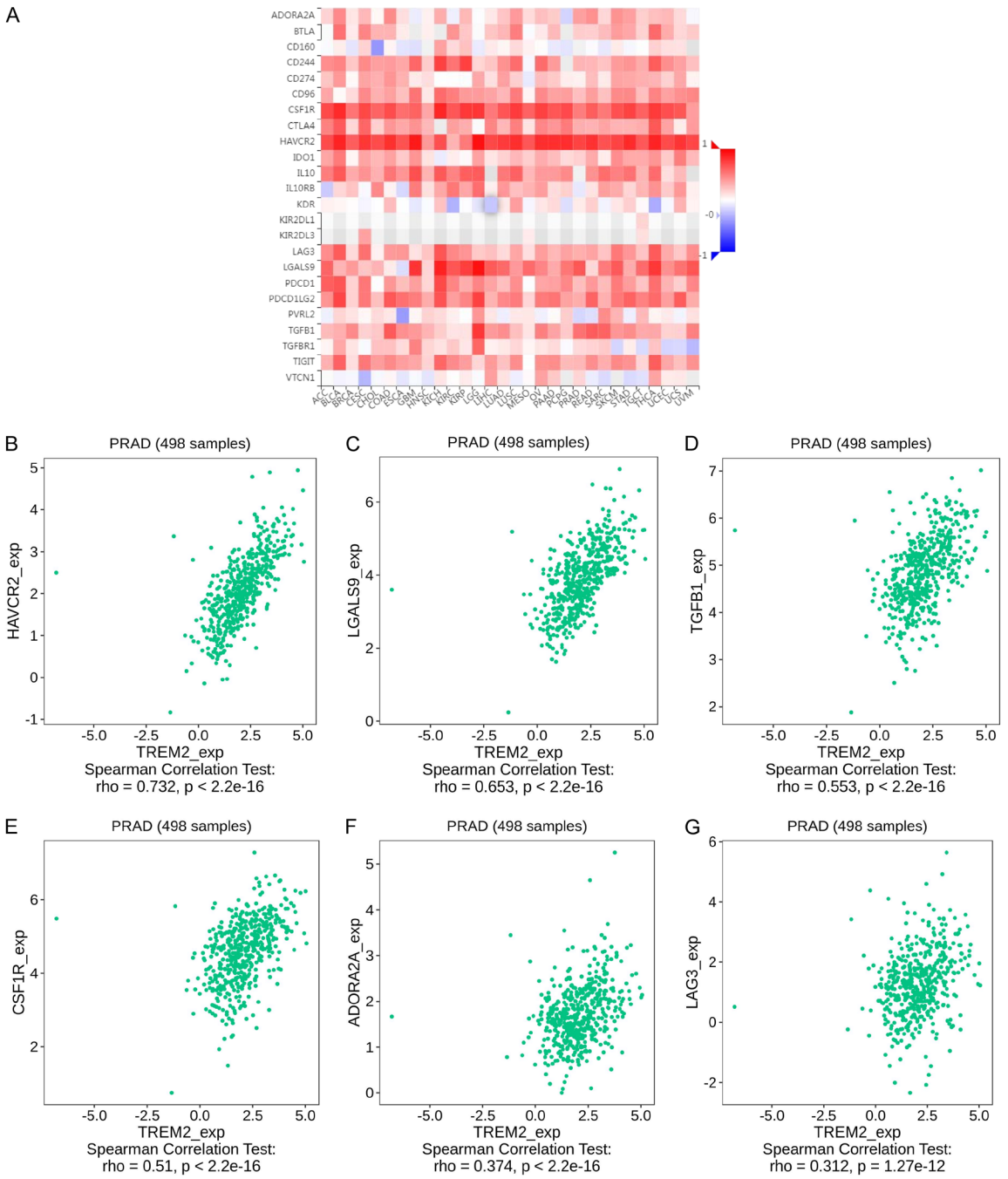

Figure 8. Analysis of correlation between TREM2 and immuno-inhibitors in PRAD. (A) Heatmap outcomes describing the associations between TREM2 and immuno-inhibitors in PRAD. (B-G) Associations between the TREM2 expression and immuno-inhibitors in PRAD: (B) HAVCR2, (C) LGALS9, (D) TGF-B1, (E) CSF1R, (F) ADORA2R, and (G) LAG3. HAVCR2, the hepatitis A virus cellular receptor 2; LGALS9, Galectin 9; TGF-B1, Transforming Growth Factor Beta 1; CSF1R, Colony Stimulating Factor 1 Receptor; ADORA2R, Adenosine A2 Receptor; LAG3, Lymphocyte Activating 3.

androgen dependent prostate cancer (ADPC) to castration-resistant prostate canc (CRPC) during treatment with androgen deprivation therapy (ADT) [48]. Interestingly, PCa is highly enriched in immature myeloid DCs (iDCs), the presence of which may support tumor progression [49]. Consistent with these findings, we found that the TREM2 expression was positive-

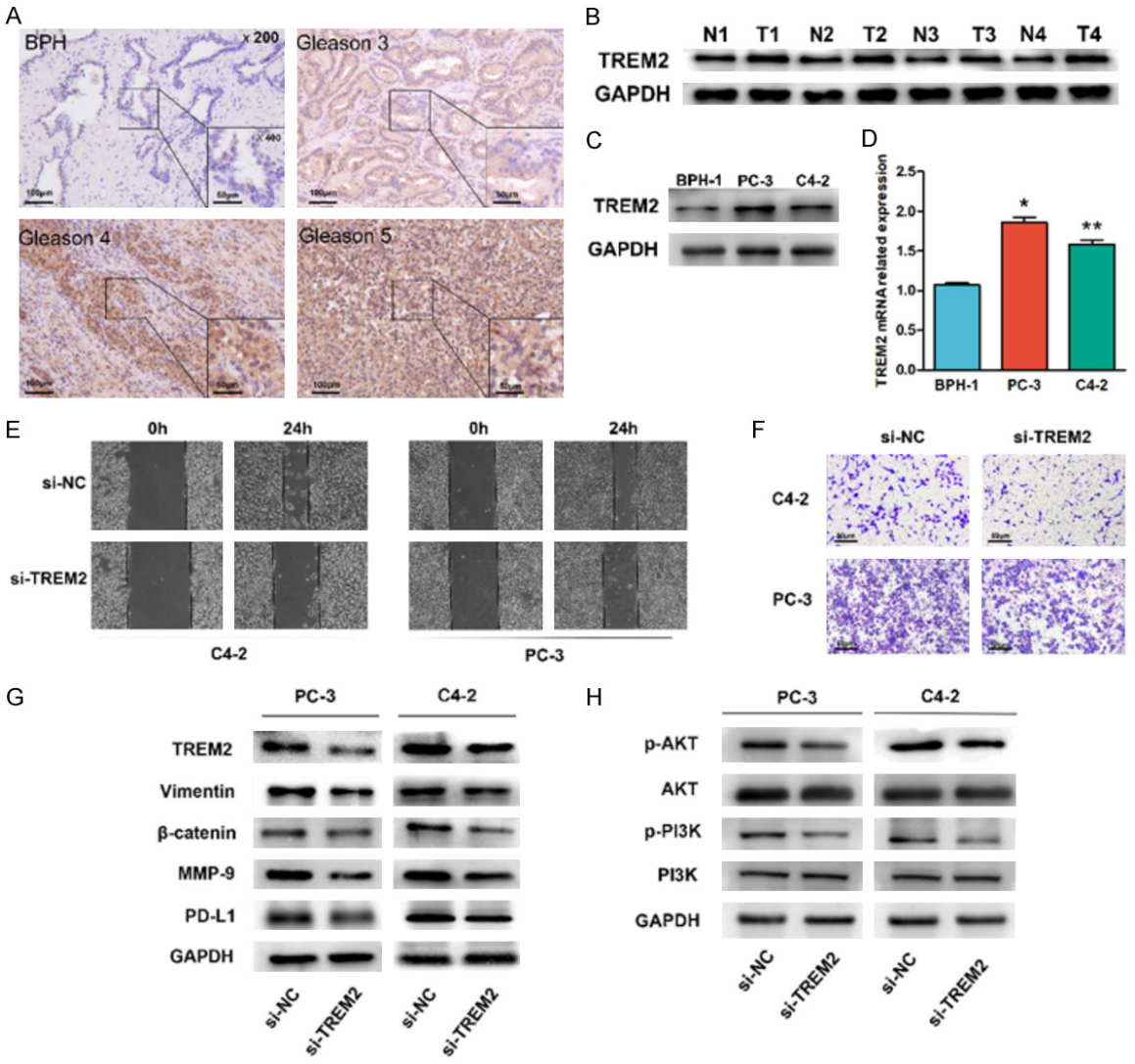

Figure 9. TREM2 knockdown inhibited the motility and invasion of PRAD cells via the PI3K/Akt pathway. A. TREM2 protein expression level in PRAD tissue samples was examined using IHC images. B. Western blot outcomes for TREM2 protein expression in four pairs of PRAD tissues. N, normal tissue; T, tumor tissue. C. Western blot outcomes for protein levels of TREM2 in various PRAD cells. D. qPCR outcomes for mRNA levels of TREM2 in various PRAD cells. E. TREM2 knockdown suppressed the migratory potentials of C4-2 and PC-3 cells. F. TREM2 knockdown suppressed the invasive ability of PC-3 and C4-2 cells. G. Western blot assay revealed that TREM2 knockdown inhibited β-catenin, MMP-9, vimentin, and PD-L1 levels in the C4-2 and PC-3 cells. H. Western blot assay indicated that TREM2 knockdown suppressed the PI3K/Akt pathway.

ly associated with the levels of infiltration by $CD8^+$ T, $CD4^+$ T, and B cells, and DCs, macrophages, and neutrophils in PRAD based on TIMER database. Moreover, TCGA-based observation also revealed correlations of higher infiltration levels with TREM2 upregulation in $CD8^+$ T cells, NK cells, B cells, DCs, and macrophages. Besides, the TREM2 expression also showed a strong correlation with the Immune Score, Stromal Score and Estimate Score. The results obtained collectively indicated that TREM2 might play an important role in regulating TIIC in the TME.

Chemokines and chemokine receptors are key regulators of the recruitment of immune cells into tumors, serving to reshape the TME immune system to a pro-tumor state [50, 51]. For example, the CCL2-CCR2 axis plays a central role in attracting immunosuppressive cells into the TME [52], and the blockade of CCL2-CCR2 hinders tumor growth, creates metasta-

sis obstacles, reduces postoperative recurrence and prolongs survival [53]. The CCL5-CCR5 axis boosts antitumor immune responses and PC progression [54], whereas the CXCL12-CXCR4 axis elicits the metastasis, angiogenesis, and viability of PCa cells [55]. In this study, we observed that there were positive associations of TREM2 with various chemokines and their receptors.

In the past decade, immunotherapy with ICIs has achieved tremendous success for treating many tumor types [56]. However, multiple clinical trials demonstrated that the ICIs yielded unsatisfactory efficacy for patients with metastatic castration-resistant PCa, with very limited survival benefit [57-59]. Recently, multiple studies have shown that TREM2 acts as a crucial signal hub mediating antitumor immunity, which is emerging as a new candidate for tumor immunotherapy. Anti-PD-1 immunotherapy has been reported to be more effective in TREM2-deficient mice than in wild-type tumor-bearing mice [27]. The findings of this study were consistent with previous findings, in that a positive association was observed between TREM2 expression and CTLA4, PD-1, and PD-L1 in PRAD samples from the TCGA database.

In *In vitro* experiments, we demonstrated the significant TREM2 upregulation in the tissues and cells of PRAD, indicating that TREM2 may facilitate prostate carcinogenesis. However, the underlying mechanism by which TREM2 may influence PRAD progression remains poorly understood. The evidence suggested that TREM2 could promote the EMT of gastric cancer via the PI3K/Akt axis [20]. Li et al. provided evidence that the proliferation and invasion of glioma cells were strengthened by TREM2 overexpression [20]. Consistent with previous findings, our results showed that the TREM2 knockdown significantly impaired the invasive and migratory ability of PC cell lines after transfection with TREM2 siRNA. Further investigations indicated that TREM2 contributed to the progression of PRAD via the EMT-mediated PI3K/Akt pathway, which was consistent with the predictive findings of the GSEA. Additionally, along with the lowered TREM2 protein levels, we observed a significant decrease in PD-1 expression, suggesting that TREM2 might participate in the immune response of PRAD via PD-L1.

Despite the aforementioned novel findings, our study has some limitations. First, we did not use an animal model to further validate the carcinogenesis of TREM2. Second, although our study observed a correlation between TREM2 upregulation and the Gleason score, it did not reach statistical significance. Therefore, further studies are needed to determine the prognostic value of TREM2 using a larger number of cases.

Conclusions

The results of this study demonstrated a significant increase in TREM2 expression in PRAD. We observed that high TREM2 expression is closely related to unfavorable clinicopathologic characteristics, indicating that TREM2 is an independent biomarker for PFI prognosis among patients with PRAD. Our data also indicated a prominent correlation between TREM2 and multiple immune marker sets, highlighting the potential of TREM2 as a modulator for the tumor immune microenvironment. Finally, knockdown of TREM2 significantly impaired the migration capability of PC cells lines via the AKT/PI3K signal pathway. In summary, TREM2 may represent a potential predictive biomarker and antitumor strategies, especially immunotherapy.

Acknowledgements

This study was partially supported by The National Natural Science Foundation of China (No. 81970216, 81972411), The Natural Science Foundation of Hebei Province (No. H2019206032).

Disclosure of conflict of interest

None.

Address correspondence to: Xiao-Lu Wang and Chang-Bao Qu, Department of Urology, The Second Hospital of Hebei Medical University, 215 Heping W Road, Shijiazhuang 050000, Hebei, China. E-mail: wxlurology@126.com (XLW); Changbao_qu@126.com (CBQ)

References

[1] Bray F, Ferlay J, Soerjomataram I, Siegel RL, Torre LA and Jemal A. Global cancer statistics 2018: GLOBOCAN estimates of incidence and mortality worldwide for 36 cancers in 185 countries. CA Cancer J Clin 2018; 68: 394-424.

[2] Erratum: global cancer statistics 2018: GLOBOCAN estimates of incidence and mortality worldwide for 36 cancers in 185 countries. CA Cancer J Clin 2020; 70: 313.
[3] Siegel RL, Miller KD and Jemal A. Cancer statistics, 2020. CA Cancer J Clin 2020; 70: 7-30.
[4] Armenia J, Wankowicz SAM, Liu D, Gao J, Kundra R, Reznik E, Chatila WK, Chakravarty D, Han GC, Coleman I, Montgomery B, Pritchard C, Morrissey C, Barbieri CE, Beltran H, Sboner A, Zafeiriou Z, Miranda S, Bielski CM, Penson AV, Tolonen C, Huang FW, Robinson D, Wu YM, Lonigro R, Garraway LA, Demichelis F, Kantoff PW, Taplin ME, Abida W, Taylor BS, Scher HI, Nelson PS, de Bono JS, Rubin MA, Sawyers CL, Chinnaiyan AM; PCF/SU2C International Prostate Cancer Dream Team, Schultz N and Van Allen EM. The long tail of oncogenic drivers in prostate cancer. Nat Genet 2018; 50: 645-651.
[5] Yan W, Jamal M, Tan SH, Song Y, Young D, Chen Y, Katta S, Ying K, Ravindranath L, Woodle T, Kohaar I, Cullen J, Kagan J, Srivastava S, Dobi A, McLeod DG, Rosner IL, Sesterhenn IA, Srinivasan A, Srivastava S and Petrovics G. Molecular profiling of radical prostatectomy tissue from patients with no sign of progression identifies ERG as the strongest independent predictor of recurrence. Oncotarget 2019; 10: 6466-6483.
[6] Hanahan D and Coussens LM. Accessories to the crime: functions of cells recruited to the tumor microenvironment. Cancer Cell 2012; 21: 309-322.
[7] Coussens LM, Zitvogel L and Palucka AK. Neutralizing tumor-promoting chronic inflammation: a magic bullet? Science 2013; 339: 286-291.
[8] Gajewski TF, Schreiber H and Fu YX. Innate and adaptive immune cells in the tumor microenvironment. Nat Immunol 2013; 14: 1014-1022.
[9] Son B, Lee S, Youn H, Kim E, Kim W and Youn B. The role of tumor microenvironment in therapeutic resistance. Oncotarget 2017; 8: 3933-3945.
[10] Pasero C, Gravis G, Guerin M, Granjeaud S, Thomassin-Piana J, Rocchi P, Paciencia-Gros M, Poizat F, Bentobji M, Azario-Cheillan F, Walz J, Salem N, Brunelle S, Moretta A and Olive D. Inherent and tumor-driven immune tolerance in the prostate microenvironment impairs natural killer cell antitumor activity. Cancer Res 2016; 76: 2153-2165.
[11] Miller AM, Lundberg K, Özenci V, Banham AH, Hellström M, Egevad L and Pisa P. CD4+CD25high T cells are enriched in the tumor and peripheral blood of prostate cancer patients. J Immunol 2006; 177: 7398-7405.
[12] Sharma P and Allison JP. The future of immune checkpoint therapy. Science 2015; 348: 56-61.
[13] Peng Q, Malhotra S, Torchia JA, Kerr WG, Coggeshall KM and Humphrey MB. TREM2- and DAP12-dependent activation of PI3K requires DAP10 and is inhibited by SHIP1. Sci Signal 2010; 3: ra38.
[14] Bouchon A, Hernández-Munain C, Cella M and Colonna M. A DAP12-mediated pathway regulates expression of CC chemokine receptor 7 and maturation of human dendritic cells. J Exp Med 2001; 194: 1111-1122.
[15] Hamerman JA, Jarjoura JR, Humphrey MB, Nakamura MC, Seaman WE and Lanier LL. Cutting edge: inhibition of TLR and FcR responses in macrophages by triggering receptor expressed on myeloid cells (TREM)-2 and DAP12. J Immunol 2006; 177: 2051-2055.
[16] Paloneva J, Mandelin J, Kiialainen A, Böhling T, Prudlo J, Hakola P, Haltia M, Konttinen YT and Peltonen L. DAP12/TREM2 deficiency results in impaired osteoclast differentiation and osteoporotic features. J Exp Med 2003; 198: 669-675.
[17] Gordon S and Taylor PR. Monocyte and macrophage heterogeneity. Nat Rev Immunol 2005; 5: 953-964.
[18] Takahashi K, Rochford CD and Neumann H. Clearance of apoptotic neurons without inflammation by microglial triggering receptor expressed on myeloid cells-2. J Exp Med 2005; 201: 647-657.
[19] Zhang H, Sheng L, Tao J, Chen R, Li Y, Sun Z and Qian W. Depletion of the triggering receptor expressed on myeloid cells 2 inhibits progression of renal cell carcinoma via regulating related protein expression and PTEN-PI3K/Akt pathway. Int J Oncol 2016; 49: 2498-2506.
[20] Li C, Hou X, Yuan S, Zhang Y, Yuan W, Liu X, Li J, Wang Y, Guan Q and Zhou Y. High expression of TREM2 promotes EMT via the PI3K/AKT pathway in gastric cancer: bioinformatics analysis and experimental verification. J Cancer 2021; 12: 3277-3290.
[21] Zhang X, Wang W, Li P, Wang X and Ni K. High TREM2 expression correlates with poor prognosis in gastric cancer. Hum Pathol 2018; 72: 91-99.
[22] Wang XQ, Tao BB, Li B, Wang XH, Zhang WC, Wan L, Hua XM and Li ST. Overexpression of TREM2 enhances glioma cell proliferation and invasion: a therapeutic target in human glioma. Oncotarget 2016; 7: 2354-66.
[23] Kluckova K, Kozak J, Szaboova K, Rychly B, Svajdler M, Suchankova M, Tibenska E, Filova B, Steno J, Matejcik V, Homolova M and Bucova M. TREM-1 and TREM-2 expression on blood monocytes could help predict survival in high-

grade glioma patients. Mediators Inflamm 2020; 2020: 1798147.
[24] Katzenelenbogen Y, Sheban F, Yalin A, Yofe I, Svetlichnyy D, Jaitin DA, Bornstein C, Moshe A, Keren-Shaul H, Cohen M, Wang SY, Li B, David E, Salame TM, Weiner A and Amit I. Coupled scRNA-Seq and intracellular protein activity reveal an immunosuppressive role of TREM2 in cancer. Cell 2020; 182: 872-885, e19.
[25] Yao Y, Li H, Chen J, Xu W, Yang G, Bao Z, Xia D, Lu G, Hu S and Zhou J. TREM-2 serves as a negative immune regulator through Syk pathway in an IL-10 dependent manner in lung cancer. Oncotarget 2016; 7: 29620-34.
[26] Lavin Y, Kobayashi S, Leader A, Amir ED, Elefant N, Bigenwald C, Remark R, Sweeney R, Becker CD, Levine JH, Meinhof K, Chow A, Kim-Shulze S, Wolf A, Medaglia C, Li H, Rytlewski JA, Emerson RO, Solovyov A, Greenbaum BD, Sanders C, Vignali M, Beasley MB, Flores R, Gnjatic S, Pe'er D, Rahman A, Amit I and Merad M. Innate immune landscape in early lung adenocarcinoma by paired single-cell analyses. Cell 2017; 169: 750-765, e17.
[27] Molgora M, Esaulova E, Vermi W, Hou J, Chen Y, Luo J, Brioschi S, Bugatti M, Omodei AS, Ricci B, Fronick C, Panda SK, Takeuchi Y, Gubin MM, Faccio R, Cella M, Gilfillan S, Unanue ER, Artyomov MN, Schreiber RD and Colonna M. TREM2 modulation remodels the tumor myeloid landscape enhancing anti-PD-1 immunotherapy. Cell 2020; 182: 886-900, e17.
[28] Thomas PD. The gene ontology and the meaning of biological function. The gene ontology handbook. Humana Press: New York, NY; 2017. pp. 15-24.
[29] Shannon P, Markiel A, Ozier O, Baliga NS, Wang JT, Ramage D, Amin N, Schwikowski B and Ideker T. Cytoscape: a software environment for integrated models of biomolecular interaction networks. Genome Res 2003; 13: 2498-2504.
[30] Yu G, Wang LG, Han Y and He QY. clusterProfiler: an R package for comparing biological themes among gene clusters. OMICS 2012; 16: 284-287.
[31] Fridman WH, Pagès F, Sautès-Fridman C and Galon J. The immune contexture in human tumours: impact on clinical outcome. Nat Rev Cancer 2012; 12: 298-306.
[32] Nonomura N, Takayama H, Nishimura K, Oka D, Nakai Y, Shiba M, Tsujimura A, Nakayama M, Aozasa K and Okuyama A. Decreased number of mast cells infiltrating into needle biopsy specimens leads to a better prognosis of prostate cancer. Br J Cancer 2007; 97: 952-956.
[33] Li T, Fan J, Wang B, Traugh N, Chen Q, Liu JS, Li B and Liu XS. TIMER: a web server for comprehensive analysis of tumor-infiltrating immune cells. Cancer Res 2017; 77: e108-e110.
[34] Griffith JW, Sokol CL and Luster AD. Chemokines and chemokine receptors: positioning cells for host defense and immunity. Annu Rev Immunol 2014; 32: 659-702.
[35] Eckert N, Permanyer M, Yu K, Werth K and Förster R. Chemokines and other mediators in the development and functional organization of lymph nodes. Immunol Rev 2019; 289: 62-83.
[36] Yoshihara K, Shahmoradgoli M, Martínez E, Vegesna R, Kim H, Torres-Garcia W, Treviño V, Shen H, Laird PW, Levine DA, Carter SL, Getz G, Stemke-Hale K, Mills GB and Verhaak RG. Inferring tumour purity and stromal and immune cell admixture from expression data. Nat Commun 2013; 4: 2612.
[37] Deczkowska A, Weiner A and Amit I. The physiology, pathology, and potential therapeutic applications of the TREM2 signaling pathway. Cell 2020; 181: 1207-1217.
[38] Kim SM, Kim EM, Ji KY, Lee HY, Yee SM, Woo SM, Yi JW, Yun CH, Choi H and Kang HS. TREM2 acts as a tumor suppressor in colorectal carcinoma through Wnt1/beta-catenin and Erk signaling. Cancers (Basel) 2019; 11: 1315.
[39] Tang W, Lv B, Yang B, Chen Y, Yuan F, Ma L, Chen S, Zhang S and Xia J. TREM2 acts as a tumor suppressor in hepatocellular carcinoma by targeting the PI3K/Akt/β-catenin pathway. Oncogenesis 2019; 8: 9.
[40] Qiu H, Shao Z, Wen X, Jiang J, Ma Q, Wang Y, Huang L, Ding X and Zhang L. TREM2: keeping pace with immune checkpoint inhibitors in cancer immunotherapy. Front Immunol 2021; 12: 716710.
[41] De Marzo AM, Platz EA, Sutcliffe S, Xu J, Grönberg H, Drake CG, Nakai Y, Isaacs WB and Nelson WG. Inflammation in prostate carcinogenesis. Nat Rev Cancer 2007; 7: 256-269.
[42] Taverna G, Pedretti E, Di Caro G, Borroni EM, Marchesi F and Grizzi F. Inflammation and prostate cancer: friends or foe? Inflamm Res 2015; 64: 275-286.
[43] Ness N, Andersen S, Valkov A, Nordby Y, Donnem T, Al-Saad S, Busund LT, Bremnes RM and Richardsen E. Infiltration of CD8+ lymphocytes is an independent prognostic factor of biochemical failure-free survival in prostate cancer. Prostate 2014; 74: 1452-1461.
[44] McArdle PA, Canna K, McMillan DC, McNicol AM, Campbell R and Underwood MA. The relationship between T-lymphocyte subset infiltration and survival in patients with prostate cancer. Br J Cancer 2004; 91: 541-543.
[45] Liu Y, Sæter T, Vlatkovic L, Servoll E, Waaler G, Axcrona U, Giercksky KE, Nesland JM, Suo ZH and Axcrona K. Dendritic and lymphocytic cell infiltration in prostate carcinoma. Histol Histopathol 2013; 28: 1621-1628.

[46] Nonomura N, Takayama H, Nakayama M, Nakai Y, Kawashima A, Mukai M, Nagahara A, Aozasa K and Tsujimura A. Infiltration of tumour-associated macrophages in prostate biopsy specimens is predictive of disease progression after hormonal therapy for prostate cancer. BJU Int 2011; 107: 1918-1922.
[47] Fujii T, Shimada K, Asai O, Tanaka N, Fujimoto K, Hirao K and Konishi N. Immunohistochemical analysis of inflammatory cells in benign and precancerous lesions and carcinoma of the prostate. Pathobiology 2013; 80: 119-126.
[48] Gannon PO, Poisson AO, Delvoye N, Lapointe R, Mes-Masson AM and Saad F. Characterization of the intra-prostatic immune cell infiltration in androgen-deprived prostate cancer patients. J Immunol Methods 2009; 348: 9-17.
[49] Banchereau J and Palucka AK. Dendritic cells as therapeutic vaccines against cancer. Nat Rev Immunol 2005; 5: 296-306.
[50] Chow MT and Luster AD. Chemokines in cancer. Cancer Immunol Res 2014; 2: 1125-1131.
[51] Nagarsheth N, Wicha MS and Zou W. Chemokines in the cancer microenvironment and their relevance in cancer immunotherapy. Nat Rev Immunol 2017; 17: 559-572.
[52] Huang B, Lei Z, Zhao J, Gong W, Liu J, Chen Z, Liu Y, Li D, Yuan Y, Zhang GM and Feng ZH. CCL2/CCR2 pathway mediates recruitment of myeloid suppressor cells to cancers. Cancer Lett 2007; 252: 86-92.
[53] Li X, Yao W, Yuan Y, Chen P, Li B, Li J, Chu R, Song H, Xie D, Jiang X and Wang H. Targeting of tumour-infiltrating macrophages via CCL2/CCR2 signalling as a therapeutic strategy against hepatocellular carcinoma. Gut 2017; 66: 157-167.
[54] Huang R, Guo L, Gao M, Li J and Xiang S. Research trends and regulation of CCL5 in prostate cancer. Onco Targets Ther 2021; 14: 1417-1427.
[55] Singh S, Singh UP, Grizzle WE and Lillard JW Jr. CXCL12-CXCR4 interactions modulate prostate cancer cell migration, metalloproteinase expression and invasion. Lab Invest 2004; 84: 1666-1676.
[56] Tang J, Yu JX, Hubbard-Lucey VM, Neftelinov ST, Hodge JP and Lin Y. Trial watch: the clinical trial landscape for PD1/PDL1 immune checkpoint inhibitors. Nat Rev Drug Discov 2018; 17: 854-855.
[57] Antonarakis ES, Piulats JM, Gross-Goupil M, Goh J, Ojamaa K, Hoimes CJ, Vaishampayan U, Berger R, Sezer A, Alanko T, de Wit R, Li C, Omlin A, Procopio G, Fukasawa S, Tabata KI, Park SH, Feyerabend S, Drake CG, Wu H, Qiu P, Kim J, Poehlein C and de Bono JS. Pembrolizumab for treatment-refractory metastatic castration-resistant prostate cancer: multicohort, open-label phase II KEYNOTE-199 study. J Clin Oncol 2020; 38: 395-405.
[58] Beer TM, Kwon ED, Drake CG, Fizazi K, Logothetis C, Gravis G, Ganju V, Polikoff J, Saad F, Humanski P, Piulats JM, Gonzalez Mella P, Ng SS, Jaeger D, Parnis FX, Franke FA, Puente J, Carvajal R, Sengeløv L, McHenry MB, Varma A, van den Eertwegh AJ and Gerritsen W. Randomized, double-blind, phase III trial of ipilimumab versus placebo in asymptomatic or minimally symptomatic patients with metastatic chemotherapy-naive castration-resistant prostate cancer. J Clin Oncol 2017; 35: 40-47.
[59] Hansen AR, Massard C, Ott PA, Haas NB, Lopez JS, Ejadi S, Wallmark JM, Keam B, Delord JP, Aggarwal R, Gould M, Yang P, Keefe SM and Piha-Paul SA. Pembrolizumab for advanced prostate adenocarcinoma: findings of the KEYNOTE-028 study. Ann Oncol 2018; 29: 1807-1813.

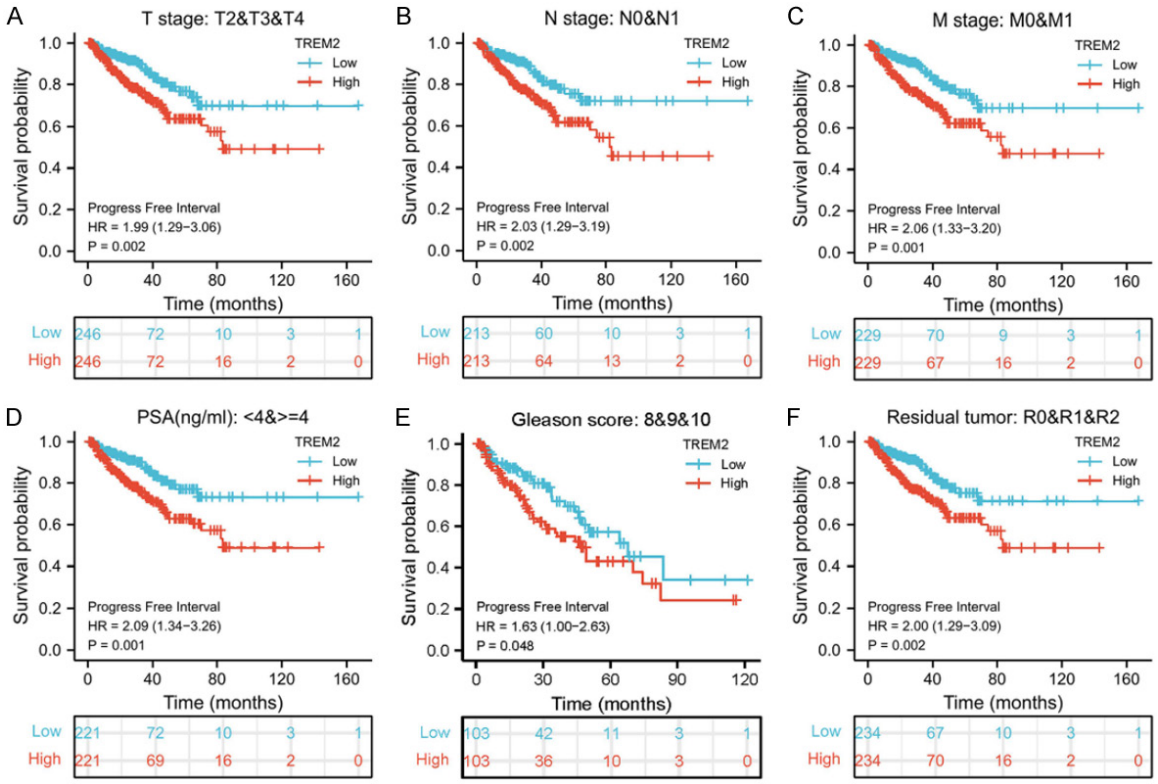

Figure S1. High-expression levels of TREM2 had a worse PFI in the subgroup of clinical features in TCGA-PRAD cohort. A. T stage; B. N stage; C. M stage; D. PSA; E. Gleason score; F. Residual tumor.

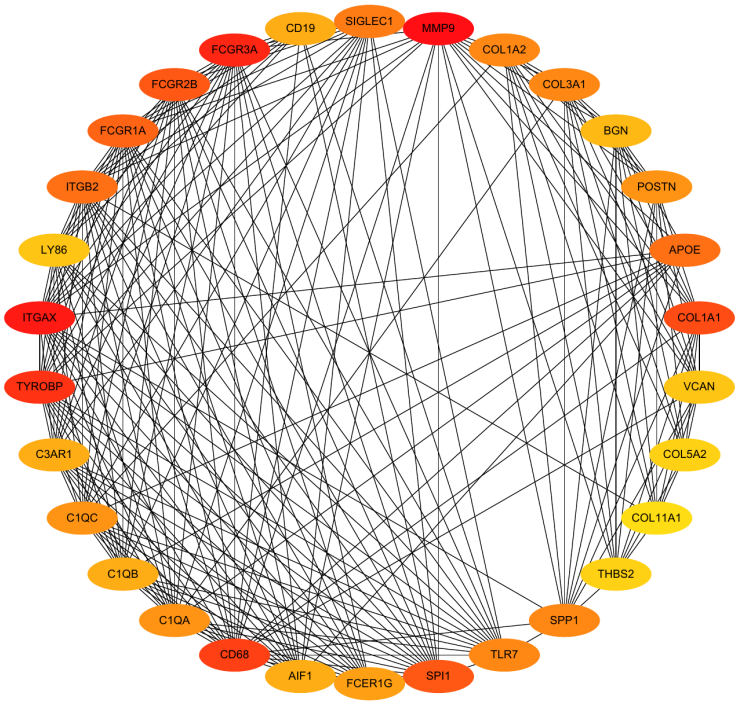

Figure S2. PPI network assessment of TREM2 in PRAD. PPI network of TREM2 was constructed using STRING.

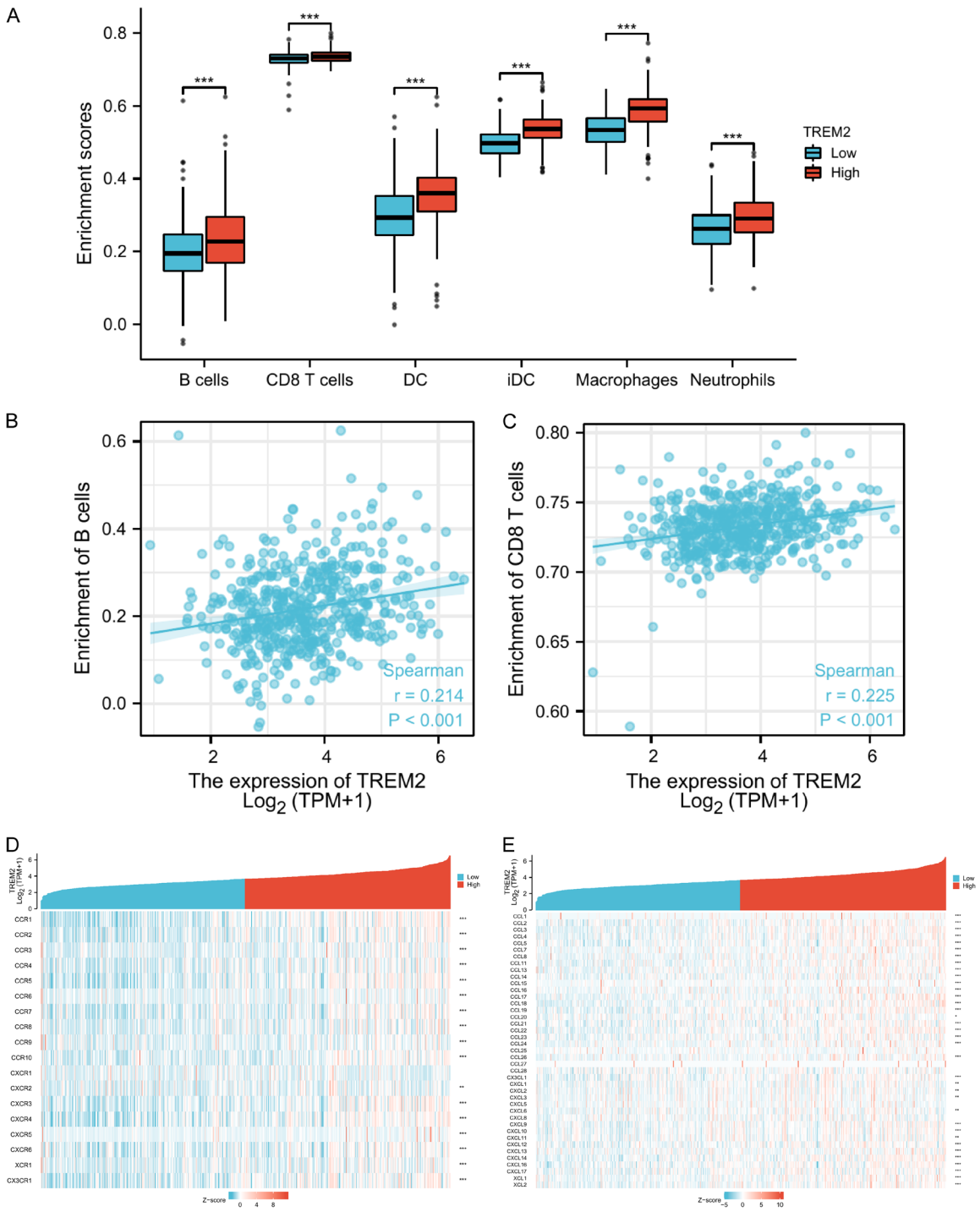

Figure S3. Association of TREM2 expression level with TIICs, chemokines and/or their receptors in PRAD. (A) Differential distributions of immunocytes among patients with downregulation versus upregulation. (B, C) Association of the TREM2 expression with the immune infiltration in PRAD: (B) B cells, (C) $CD8^+$ T cells. (D, E) Correlations of the TREM2 expression levels with chemokines and/or their receptors. (D) Heatmap outcomes describing the TREM2-chemokine receptors associations in PRAD. (E) Heatmap outcomes describing the TREM2-chemokine associations in PRAD.